Morphing Aircraft Structures

1- Introduction

Airplanes fly under a wide range of temperature, density and wind conditions. They also have to perform different flight manoeuvres during a flight. The aircrafts are designed to have the best performance in the most important flight stage, which depend on the mission that the aircraft have to accomplish. When they fly out of the optimal flight condition, the performance is severely affected.

Although fixed wings must operate under the design condition, this is not possible often, especially in aircrafts which have a wide operating range, like surveillance and military aircrafts. For commercial aircrafts during takeoff, landing and other short flight stages, high-lift devices are used to improve the performance.

Nowadays, researches are being conducted to create airplanes' structures that may radically change their shape in-flight, in order to get the best aircraft shape for the given flight condition. The aircrafts will be able to operate in optimal conditions throughout the entire flight envelope, which will increase their fuel efficiency and manoeuvring capabilities. These aircrafts are called "morphing aircrafts".

So far, new concepts never have gone further than the experimental state due to the high complexity of structures, the lack of energy efficiency as well as the weight efficiency of the actuation devices. Recently, new technologies and the creation of advanced materials made possible the design of morphing wings that can adapt to a specific flight condition in order to improve the aircraft performance.

The aircraft's performance can be improved by adjusting the span, chord and sweep angle among others. It is important to choose the right parameters to adjust because some may cause undesirable side effects on the performance, others don't change significantly the performance. It is required to know which parameters affect mostly the performance; these parameters are airfoil shape and wing planform. Altering the wing planform changes numerous parameters like span, chord, sweep, dihedral and twist angles; while altering the airfoils shape, changes the thickness and camber line.

Morphing structures are complex and require several actuation devices, which increase aircraft weight. Manufacturing is thus harder than in fixed wings. As a result, it's necessary to balance the improvement of performance with the increase of complexity and weight.

2- Specific Background

The aerodynamic analysis is done in two steps. First, the 2-dimensional (2D), then, a non-linear lifting-line method algorithm is used to obtain the lift distribution and induced drag. The lift and the parasite drag are obtained by integrating the lift and parasite drag coefficients corresponding to all local angles of attack.

A total of 13 design variables are adopted in this design problem. In this case, the span is allowed to vary between 2.4m and 3.4m and the chord length is limited to a minimum of 0.22m and a maximum of 0.33m. There is no twist of the wing since the morphing concept does not permit such mechanism and the sweep angle at quarter chord position is kept constant and equal to zero.

The aim of the optimization is to minimize the drag of the wing at speeds between 15m/s and 50m/s. The lift required is the UAV weight of 100N.

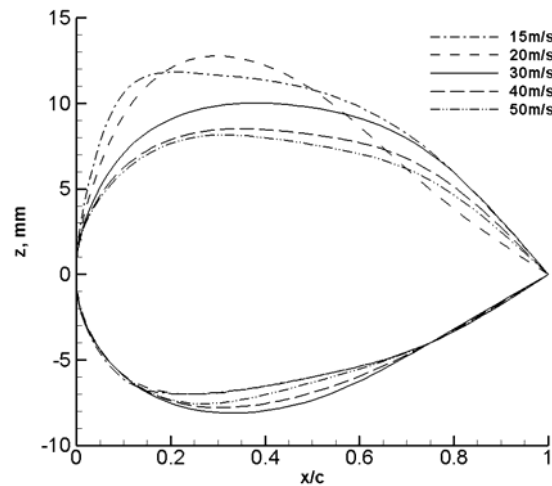The airfoil resulting from the optimization process is shown in the next figures.

Figure 1 - *Airfoil sections and wing planforms for five speeds*

In order to achieve the desired shape changes for the morphing wing, the skin material has to endure high strains, which is not the case with the materials usually used in conventional aircraft. Vulcanized rubber was chosen to be the skin material, due to its availability, low price and the desire to prove the feasibility of the morphing concept without much concern about cyclic fatigue or environmental hazard.

The structural model must not only be capable of increasing the chord at a wing section but also of discretizing the airfoil and allowing changes in airfoil thickness at some control points. In this work, it is considered that the mechanism divides the airfoil in 6 different sections along the chord. The span expansion mechanism is intended to stretch the wing skin and also maintain the rib expansion mechanisms evenly distributed along the span of the wing.

The finite element method (FEM) structural model of the wing was built not only to perform the coupled aerodynamic-structural analysis but also to assess the wing deformation forces involved in such a structure.

Rubber like materials can be modelled in a number of ways when a FEM is applied, traditionally, using a strain energy function dependant only on deviatory deformations.

A variety of strain energy functions are supported by Ansys®, the commercial structural analysis program.

Aerodynamic loads are applied directly to the skin nodes as forces in the Cartesian reference frame. Since the aerodynamic mesh is different from the mesh used for the structural analysis (which is more refined), then forces in a particular location are evenly distributed around the surrounding skin nodes.

The process used to estimate the morphing wing drag and structural requirements is illustrated in figure 2. At a given flight condition and aircraft weight, the aerodynamic optimization tool optimizes the wing shape and passes it together with the aerodynamic loads to the structural model. Here the structural control points are made coincident to the aerodynamic control points and the aerodynamic loads are distributed to the skin FEM nodes. Then, the structural analysis is carried out with the control points fixed and the deformations of the skin are obtained. In the next iteration, the new wing shape is passed to the aerodynamic solver and new loads are computed. The process is repeated until convergence is achieved.
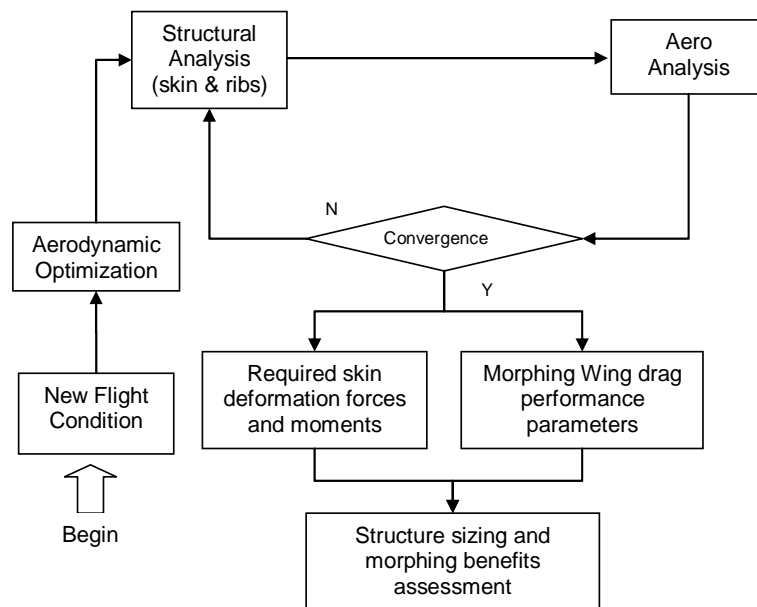

Figure 2 - *Flow chart of coupled aero-structural analysis of an optimum morphing wing at different flight speeds*

Since rubber is not a rigid material, when it is wrapped as a sleeve around the wing internal mechanism and structure with some level of pre-extension it tends to the shape shown in figure 3. Straight lines form between consecutive control points at any section and the chord and thickness reduce between consecutive ribs. As a result, the wing aerodynamic characteristics are different from the perfectly smooth optimized wing. The solution from the aero-structural analysis is shown in figure 3.

Initially, a somewhat low pre-extension value was used in the skin model. Since the control points do not move for a given configuration, the surface of the airfoil exhibited undesired bumps between the control points due to the suction that exists around the airfoil. In figure 16, the airfoil for 40m/s clearly illustrates this effect. For the other speed cases, a higher pre-extension value of the rubber has already been used which

enabled a more fixed shape with almost straight lines between control points. The pressure coefficient distributions around the wing illustrate the peaks of alternating zones of low pressure and high pressure that occur due to the small curvature of the wing surface at the control points.
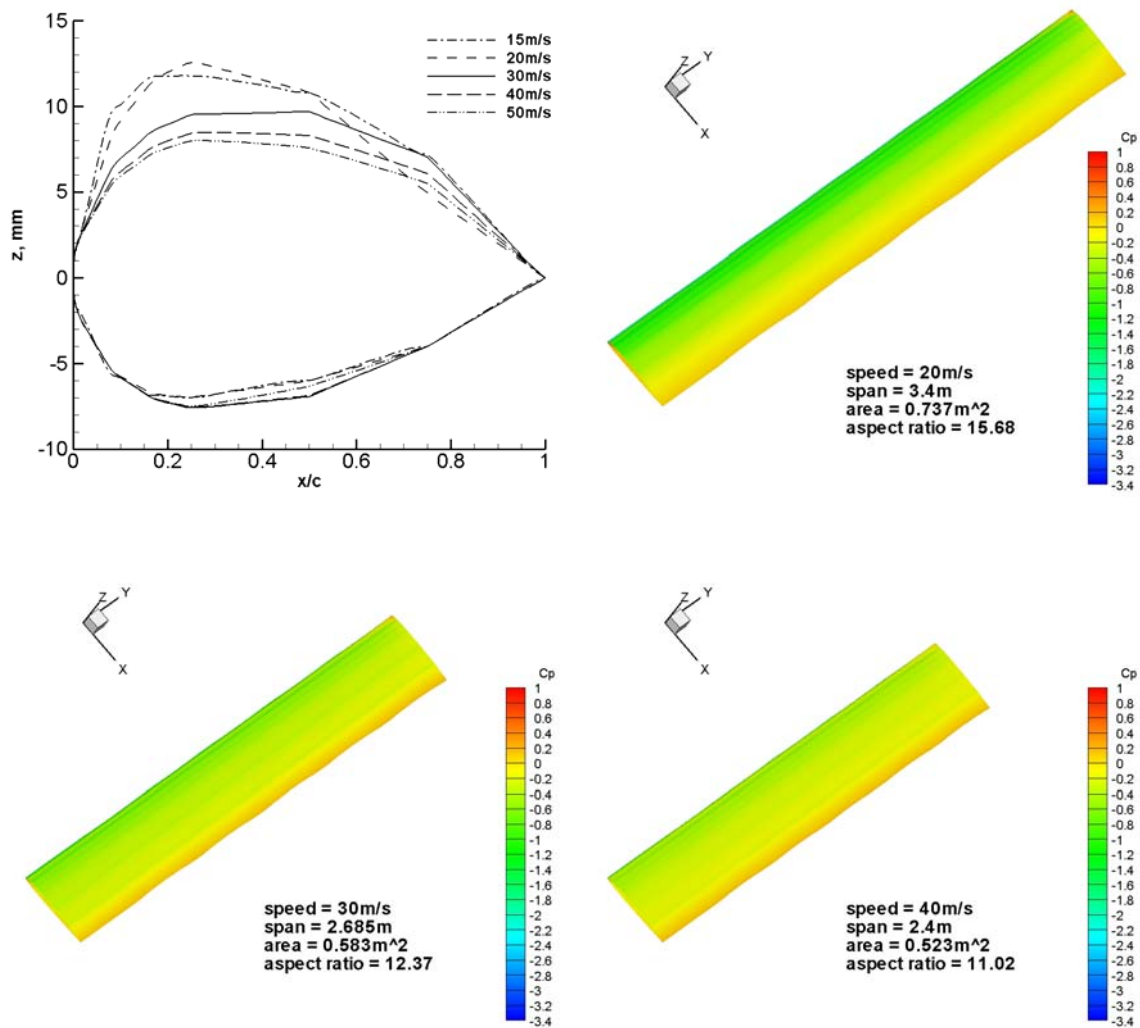

Figure 3 - *Airfoil sections at wing tip and wing planforms for five speeds from the aero-structural analysis*

When comparing the optimized morphing wing with the original wing drastic drag reductions are obtained at all speeds. At the original wing cruise speed of 30m/s, drag has reduced by more than 50%. The morphing wing design, despite its shortcomings at low speeds due to the limited thickness changes that can be produced.
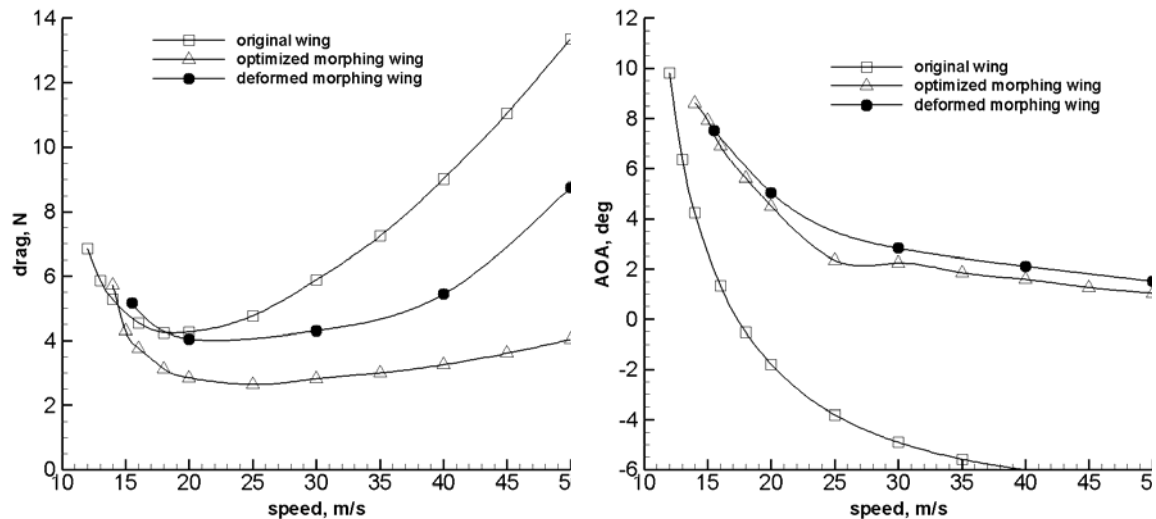
Figure 4 - *Comparison of drag and angle of attack estimates of the original wing, the optimized morphing wing and the deformed morphing wing for various flight speeds*

As anticipated, the performance of the deformed morphing wing is not so good. The skin surface deformation greatly influenced the parasite drag of this wing. The drag improvements are about half of those of the optimized morphing wing. For instance, at 30m/s the reduction in drag is 26.9%. There is a quite important shortcoming at low speed.

One important advantage of the morphing wing is that the angle of attack between 25m/s and 50m/s varies only by 1.3deg. This situation helps in maintaining the fuselage in an almost horizontal position for most of the speed range in straight and level flight, which for some surveillance applications may be of interest. On the other hand, fuselage drag can be reduced since it may be at a small angle of attack to the airflow.

3- Structural Design | Wing

The aim was to conceptualize a mechanism that allows chord and span to change, trying to approximate all possible wing planforms between the smallest area wing and the maximum area wing. Tapered and elliptical approximations are also possible to perform.

Minimizing weight is, definitely, very important in aerospace engineering but the main goal in this work is to assess whether the morphing concept works. Figure 5 shows the scheme of possible configurations.
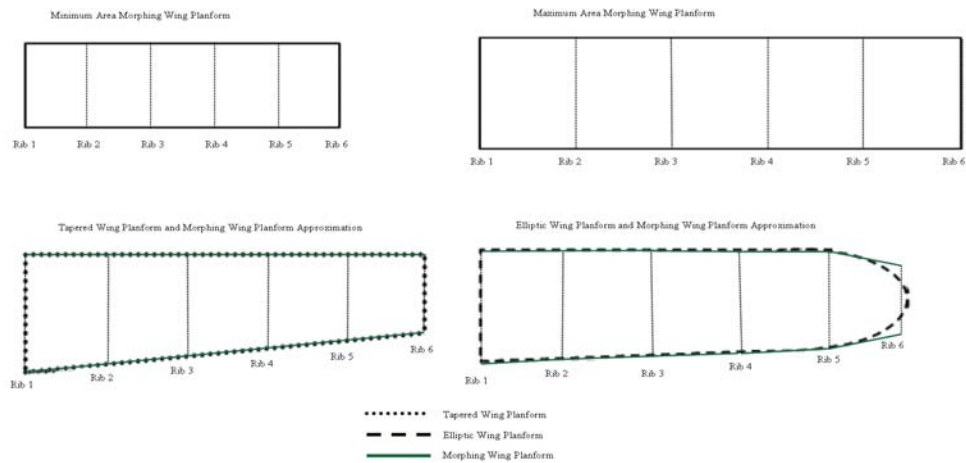
Figure 5 - *Morphing Mechanism conceptual capability*

Each chord expansion mechanism is independently actuated and allows different planform shapes to be obtained. At each rib section, independent servo-actuators are used to extend the chord in the leading edge and in the trailing edge directions, so that the quarter chord line can stay perpendicular to the wing root section.

The structural FEM model produced the following results in terms of forces for a morphing wing with the capabilities described in the previous chapter in its fully extended position: the compressive force span wise is 8000N, compressive force chord wise is 1500N and compressive force along thickness 250N.

These total forces refer to the full scale half wing, which in its retracted state is 1m long span wise, 0.22m long chord wise and has a 0.002m thick rubber skin. In order to be possible to fit the model in the wind tunnel testing facility the model has to be reduced to half size. Therefore, span is 0.5m and chord is 0,11m. In order to reduce the actuation forces needed to deform the wing skin, the skin thickness was reduced to 1mm.

The wind tunnel model is assumed to increase span and chord in the proportions used for the full scale FEM model, which are 50% increase in span and chord dimensions. Therefore, the stresses levels on the skin must be caused by the mechanism and are the same of the full scale model.

The forces in the half scale model with half skin thickness are four times smaller relative to the full size model. For the forces in the wing thickness direction, the reasoning is slightly different since it depends on the wing sections' relative thickness.

Consequently, the sizing of the half scale wing model for wind tunnel testing is based on the following actuation forces: span wise force is 2000N, chord wise force is 375N and along the thickness the force is 125N.

Since the half scale wing dimensions are very small, the thickness of the wing sections doesn't allow the design of an economically and technically feasible airfoil morphing mechanism. Because of this, changing the wing airfoil thickness was discarded and only chord and span changes were considered for the morphing mechanism design.

In this design, a fixed block in each rib supports the whole rib structure and connects the whole mechanism with the spars while screws make translation motion through the

block core and stretch the wing skin. The block also supports the nuts which are mated to the screws and are the only moving parts of the rib, since they are rotationally actuated to cause the screws translation motion.
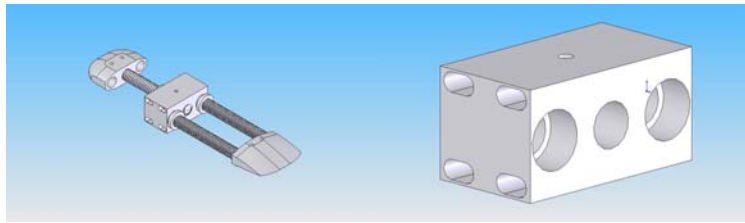

Figure 6 - *Rib parts: on the left assembled rib expansion mechanism; on the right central block*

As it happens with the leading and trailing edge blocks, the function of these extendable beams is to maintain the leading and trailing edge shape in the wing sections between ribs. The beams are connected to the leading and trailing edge block through hinges to allow taper in the wing sections between ribs, shown in figure 6.

With this design, each rib is actuated independently through the use of chains that rotate the screw nuts. This will allow greater freedom in obtaining the optimized wing planform shape, although it will increase wing weight (figure 7).
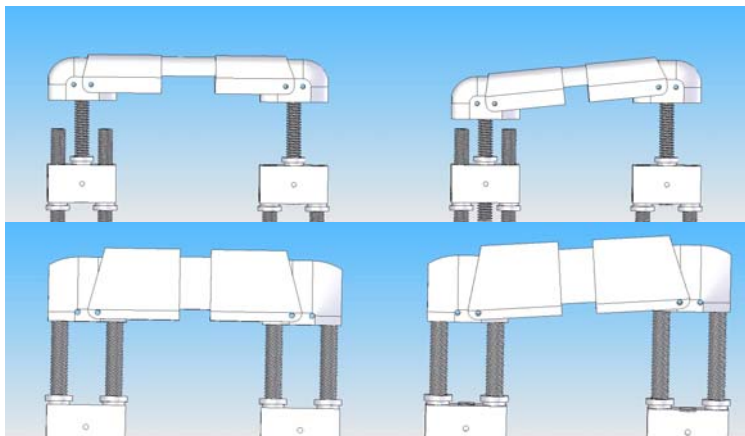

Figure 7 - *Leading and trailing edge beams assembly with the rib expansion mechanisms:*
top left: straight leading edge assembly; top right: tapered leading edge assembly; bottom left: straight trailing edge assembly; bottom right tapered trailing edge assembly

The span extension mechanism is based on beams that are pulled through the use of actuation which can be manual or motorized, rotating nuts that pull the actuation plate (the cross shaped plate) and make it slide along the threaded beams on figure 8, stretching the wing skin.
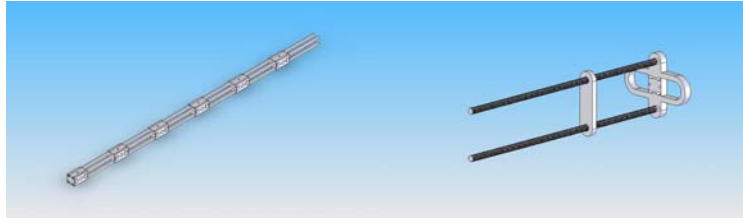
Figure 8 - *Span extension mechanism: on the right: spar expansion mechanism and on the left span actuation mechanism*

In order to extend the wing span, the wing spars must be pushed in the spanwise direction. Thus, an actuation mechanism was designed based in screws, nuts and rubber bands. This mechanism ensures a uniform space between ribs by using the rubber bands to connect them. If all rubber bands have the same elastic constant, the same displacement will cause the same reaction force for all rubber bands that keep the spacing.

The actuation plate pushes the spars and is supported by the threaded shafts that are fixed to the wing root cross-shaped plate. The horizontal extensions of the root plate are used for clamping the wing skin. The complete mechanism assembly is shown in figure 9.

Figure 9 - *Complete assembly of the morphing wing structure*

The first mechanism parts to be sized are the critical elements that support direct loadings and produce the motion of the mechanism. Those parts include the rib threaded shafts, the spars and the spars actuation mechanism threaded shafts. Other important parts are the tip, root and actuation plates, since they will be subject to the same loads as the previous parts. Although in this case no buckling is of concern. These parts were analyzed and sized based on the FEM results alone to make sure that the allowed stress was not exceeded. The rotating rib nuts and the actuation mechanism nuts were sized analytically. This comprised the definition of the necessary threaded length of the nuts to support the loadings and also the necessary nut thickness. FEM analysis were then used to confirm stress levels on the nuts unthreaded thickness. Also the gearing of the nuts were done analytically. The remaining parts (central block, leading edge and trailing edge blocks and beams) were sized based on the wing geometry. Due to their higher dimensions FEM analysis were made only to confirm stress levels. Finally, the pins that are used to connect some of the mechanism parts (leading and trailing edge blocks connect with the leading and trailing beams) were sized to withstand pure shear in the connection surface.

In order to simplify the analysis, the threads of the various threaded parts were not included in any of the FEM analysis mentioned above.

For the calculation of the actuation torque needed for rib and actuation nuts we calculate the torque needed to raise a load supported by a fastened screw. This calculation is based on the following expressions [20]:

$$M = F \frac{d_p}{2} \left[\frac{\left(\cos\left(\frac{\theta_n}{2}\right) \tan(\beta) + f \right)}{\cos\left(\frac{\theta_n}{2}\right) - f \tan(\beta)} \right] + FR_m f' ; \qquad (1)$$

$$\frac{\theta_n}{2} = a\tan\left[\tan\left(\frac{\theta}{2}\right) \cos(\beta) \right]; \quad (2)$$

$$\beta = a\tan\left(\frac{p}{\pi d_p} \right); \qquad (3)$$

The first term of the equation 1 represents the necessary torque to overcome the friction between the threads of the screw and nut while the second term represents the necessary torque to overcome the friction between the nut and the support surface where the nut lies on. Equation 2 relates the angle between the reaction force and the axis of the screw with the screw parameters θ and β, where θ is the thread profile angle and β is given by equation 3. Results for the maximum torque are shown in table 1.

Part	Material	Total Load, N	p, mm	d_p, mm	θ, °	f	f'	M, Nm
Rotating rib nut	Aluminium	489	2	7.99	29	0.3	0.3	1.49
Actuation nut	Aluminium	1250	5	9.24	29	0.3	0.3	5.47

Table 1 - *Rotating rib and actuation nuts torque requirements*

Construction of the designed mechanism took place at I.S.T mechanical laboratory for mechanical tooling. The main tool used was the milling machine. This machine has six degrees of freedom, three rotations and three translation degrees and a digital position indicator, which allows precision until centesimo of millimetre. This tool has revealed to be very powerful, since its six degrees of freedom allowed to machine all the parts of the wing structure and make the final assembly. The milling machine had recesses in the gears, so the precision of the work was less than expected.

The available tooling machines allowed a limited precision in making holes and keeping the alignment of the relatively great number of pieces to be manufactured. As a consequence, the spar extension mechanism used to equalize the distance between ribs as the span increases revealed to be extremely ineffective. Other affected parts that due to alignment difficulties couldn't withstand the loading were the expanding beams from

both the leading and trailing edge. The torsional stiffness of the eight spars was also very low, because the tolerances involved were not able to constrain the eight spars to act as a single spar. Finally, the friction force between the rotating rib nuts and the central block was very high, both in the initial requirements and in the actual mechanism assembly.

The screws and the rotating nuts were made by an exterior technician. We made the order specifying the screws' pitch and exterior diameter. For the nuts we specified exterior dimensions to fit these nuts in the central blocks (figure 10).

Figure 10 - *Shaft and rotating nut*

All other parts were made by us, using the milling machine. The leading and trailing edge beams were made with a folding machine. All the other parts of the wing were made in the milling machine (figure 11).

Figure 11 - *Leading and trailing edge sliding beams*

The interior parts of the leading and trailing edge were made at the milling machine as well as the leading and trailing edge blocks. The inclined surfaces were made by using one of the rotations of the milling machine

The central blocks were made using a cylinder of 25mm of diameter. The milling machine was used to create the rectangular shape of the crossing section of 22x24mm. Then the holes were drilled. The chord wise holes were easy to make. The holes in span direction were not so easy to drill, because these holes are deep and the driller has to be longer. Once it is hard to have a perfectly balanced drill, the drill's tip vibrations make it impossible to keep the holes aligned (figure 12).

Figure 12 - *Central block*

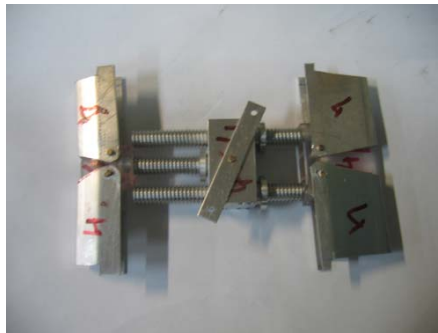The resulting rib is the one in the next photo.

Figure 13 - *Assemble rib*

The wing accomplished the entire requirements pre-established and allowed the chord and the span to vary. The next photos are the wing fully extended in the left side and the fully retracted in the right side (figure 14).
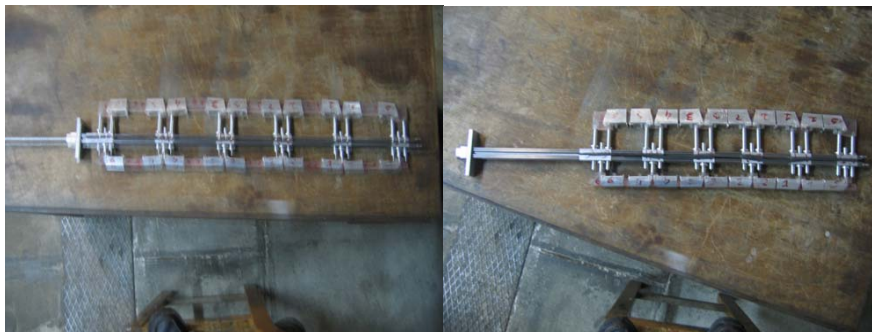

Figure 14 - *Assemble wing: in the left: extended; on the right: retracted*

The span extension mechanism equalizer was substituted by rubber bands connecting the neighbouring ribs. This solution, although dependable on the stiffness of the rubber

bands used and the friction between the central blocks and the spars, worked quite well for the precision required and resulted in wing weight loss.

Dropping the requirement of making the mechanism able to produce different wing planform shapes than rectangular and tapered shapes allowed the expanding leading and trailing edge beams to be substituted by solid sliding beams with the leading and trailing edges shapes, respectively.

The eight spars were substituted by a long U shaped plate which greatly increased the torsional stiffness, because it could be made in a whole piece by bending the plate in the desired shape.. The spar was now over dimensioned for the rubber stretching force requirements and with this change there was a weight increasing. In order to reduce the actuation force requirements, two different measures were taken: the friction surface of the rotating rib nuts was reduced by diminishing their length L_e, avoiding contact of the lower surface of the rib with the central block and at the same time reducing the contact area around the nut

In conclusion, some of the parts described previously were found to be useless; such were the tip plate, the excessively over dimensioned cruciform root plate and the double shaft mechanism for the span extension. Figure 15 shows the final mechanism assembly, which can be compared to the one of figure 14.

Figure 15 - *Final mechanism assembly*

Because of these changes in the mechanism design, the final dimensions of the prototype in the chord dimension had to be slightly changed, in the smallest chords, from 0.11m to 0.12m. However, there is still an increase in the chord and span, in 50% of their smallest dimensions. Table 8 summarizes the final prototype dimensions and its span and chord range, as well as the relative thickness variations, possible maximum thickness relative chord position variations and taper ratio range.

The new skin material was conceived having in mind some requirements. In order to allow the study of the morphing wing benefits and also understand the behaviour of a wing covered with a flexible material: it should allow high levels of strain and the manufacturing process should be such that the stiffness of the material could be changed, either through the increase of material thickness, constitution or both.

Given the resources available, we chose, after some preliminary experiments, to use licra fibre, which allows high strains of over 150%, inserted into a matrix of silicone that allows very high strains and is impermeable to air. The number of fibre layers and the amount of silicone used serve to control the stiffness of the material which is manufactured.

Figure 16 - *Licra fibre in silicone matrix composite material for the wing skin*

4- Wind Tunnel Test

Wind tunnel testing took place at AFA aeronautical laboratory facility. A blow-down wind tunnel with closed circuit was used. The balance to measure aerodynamic forces and moments was fixed at the centre of the working section. Thus an adaptation had to be made in order to install the half span wing prototype. Since this work is focused on drag and lift and their relation on the morphing wing, there was no need to calculate the transfer of moments through the supporting structure that was assembled to place the wing root aligned with the wind tunnel wall.

The supporting structure consisted of a bended beam clamped at the scale to act as an arm and place the wing root to the side of the wind tunnel test section.

To avoid interference of this structure with the airflow and therefore prevent measuring structure drag along with wing drag, a table was used over it. For the same reason, a plate with a hole was placed aligned with the wind tunnel section side. The morphing wing was connected to the supporting structure outside the wind tunnel section and inserted into the test section through the hole in the side plate. Figure 17 shows the testing assembly.

The use of the bottom and side plates incurred in some lift corrections because of ground effect and mirror effect. The side plate causes the lift to increase to double as it works as a mirror for the airflow and the bottom plate causes an increase in lift depending on the proximity of the wing to the plate.

The lift corrections are needed in order to assess the amount of lift that the wing is expected to produce, to allow a direct comparison between morphing wing configurations and the original UAV wing.

Dimensional analysis between areas is used to calculate the lift which the prototype wing is supposed to produce. From this point, the lift produced by the morphing wing with any planform configuration should be the same. The lift corrections are then calculated for each planform configuration to assess the points that should be searched for in terms of lift and drag for drag performance comparison at different wing configurations. Table 2 shows the area and expected lift for the prototype wing.

Wing	b, m	c, m	Area, m^2	A	L, N
Original	2.4	0.33	0.792	7.273	100.00
Original without Fuselage	2.0	0.33	0.660	6.061	83.33
Prototype	1.0	0.18	0.180	5.556	22.73

Table 2 - *Lift relations between original and scaled wing*

Five planform shapes of the morphing wing have been tested. The first four configurations' sequence is consistent with the optimization results obtained previously, as can be seen in table 3, where the four configurations' planform dimensions and lift corrections are given. These results show the wing tending to its maximum area configuration at low speeds, changing to tapered form at maximum span, lowest chord and maximum span and finally lowest chord and lowest span as speed increases.

Configuration	b, m	c_{Tip}, m	C_{Root}, m	Area, m^2	h/b	L/L_{Ref}	L, N
1	1.5	0.18	0.18	0.270	0.227	1.132	25.73
2	1.5	0.12	0.18	0.225	0.227	1.132	25.73
3	1.5	0.12	0.12	0.180	0.227	1.132	25.73
4	1	0.12	0.12	0.120	0.34	1.098	24.95
5	1	0.18	0.18	0.180	0.34	1.098	24.95

Table 3 - *Tested configurations' geometries and expected lift*

Wind tunnel tests were also performed to determine the influence of the initial stretch of the wing skin and its rigidity in the wing aerodynamics. The different skins were tested at configuration 4. This configuration has the smallest wing planform and therefore the skin isn't so stretched. Consequently, if the skin has not instability problems for the entire speed range, these problems will not come up if we use a bigger wing. Since the objective was to evaluate the different skins, none of the measurements taken were corrected due to the influence of the walls near the model, because all of then had the same influence.

5- *Results Analysis*

During the tests, several observations were made: the flexible skin deforms due to the pressure field of the flow; the deformation becomes higher at higher airspeeds and as the speed increases the pressure decreases carrying to higher deformations; over certain airspeed the vibration of the skin produced noise and cyclic deformations.

These observations leaded us to the study of the influence of the skin stretch and skin stiffness, on the aerodynamics of the flexible skin wing. Therefore, using the morphing

wing at configuration four, experiments were made with the wing stretched at two different expansions and also with a skin made of a double number of lycra fibre layers and with a double overall thickness. Table 4 presents the skins characteristics.

Skin	Spanwise stretch	Chordwise stretch	Nº of licra fibre layers	Thickness, mm
1	1.05	1.325	2	1
2	1.29	1.25	2	1
3	1.05	1.325	4	2

Table 4 - *Tested skins characteristics*

The testing of different wing configurations was done using skin 3. This skin was the one that maintained a reasonable performance at higher speeds, allowing a wider range of airspeeds for comparisons between wing configurations.

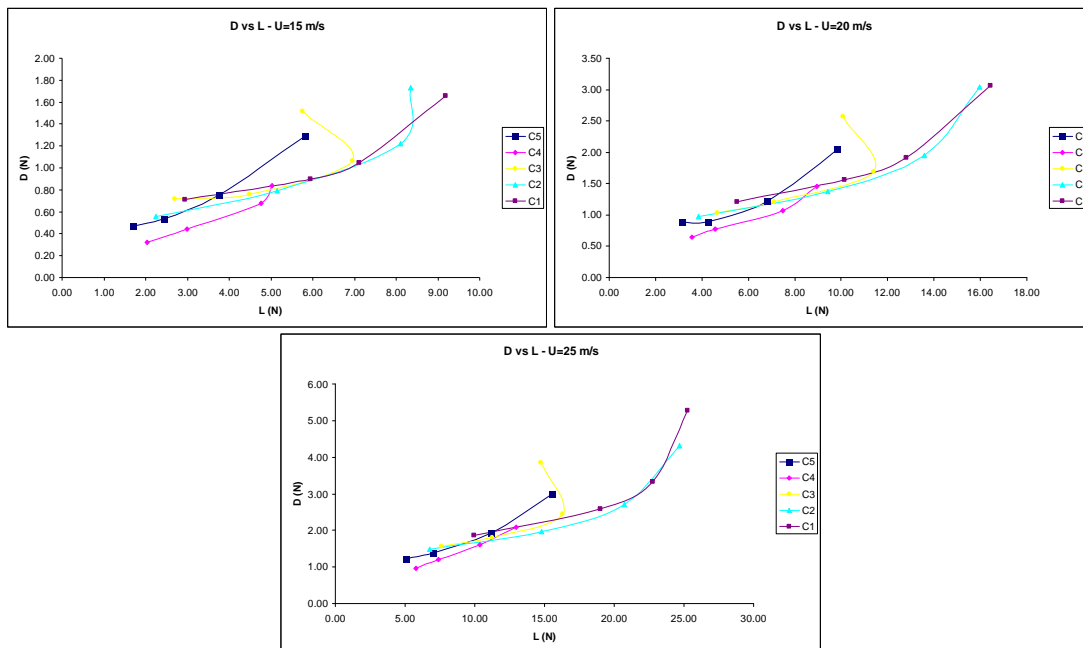The tested configurations produced the following results depicted in figures 17 and 18.

Figure 2 - *Drag versus lift curves for 15, 20 and 25 m/s airspeeds and wing planform configurations*

From the graphics above (figure 17), configurations 3, 4 and 5 do not produce the necessary lift, of about 25N, at speeds below 35m/s and configuration 1 and 2 do not produce the necessary lift at speeds below 25m/s.
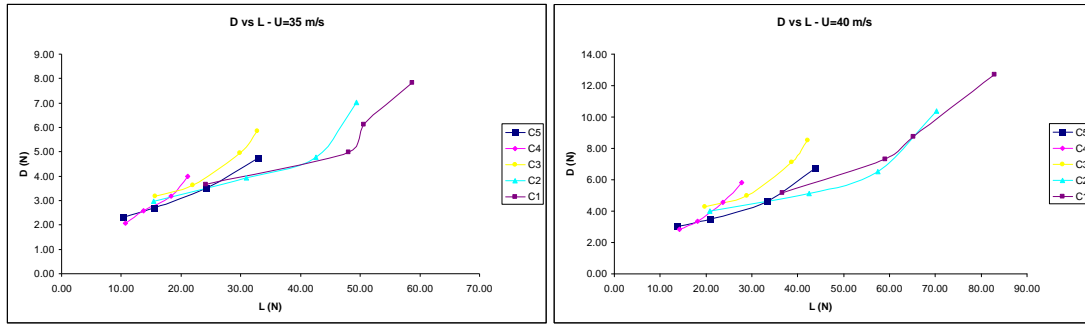
Figure 18 - *Drag versus lift curves for 35 and 40 m/s airspeeds and wing planform configurations*

Consequently, the stall speed of the morphing wing for the fully loaded UAV would be around 25m/s.

The reduction of the necessary lift that the wing is supposed to produce obviously decreases the stall speed. Depending on the required lift, the configurations that are most advantageous at different speeds may vary. Tables 5 to 7 show the drag values obtained from the drag versus lift curves by interpolation, for different values of lift.

Configuration	Lift (N)	Drag (N)		
		U=40m/s	U=35m/s	U=25m/s
1	25.73	4.92	3.74	5.74
2	25.73	4.18	3.57	4.56
3	25.73	4.51	4.11	
4	24.95	4.90	5.00	
5	24.95	3.65	3.37	

Table 5 - *Morphing wing drag for different planform configurations at different airspeeds for a 22.73 N required lift*

From the results shown above we can see that choosing to start the flight with the wing at configuration 2 at 25m/s, we can obtain a drag reduction of 12.6% at 40m/s, if we morph the wing to configuration 5 (table 5).

Configuration	Lift (N)	Drag (N)		
		U=40m/s	U=35m/s	U=25m/s
1	20.376	5.04	3.44	2.54

2	20.376	4.02	3.25	2.43
3	20.376	4.29	3.41	
4	19.764	3.62	3.60	
5	19.764	3.28	2.86	

Table 6 - *Morphing wing drag for different planform at different airspeeds for a 18.00 N required lift*

The same result can be obtained if the required lift is about 18N: the drag reductions at 40m/s can achieve 18.3%, as the wing is morphed again from configuration 2 to configuration 5.

Configuration	Lift (N)	Drag (N)		
		U=40m/s	U=35m/s	U=25m/s
1	15.282	5.29	3.16	2.21
2	15.282	3.93	2.96	1.91
3	15.282	4.57	3.18	2.28
4	14.823	2.89	2.64	2.43
5	14.823	3.10	2.49	2.77

Table 7 - *Morphing wing drag for different planform configurations at different airspeeds for a 13.50 N required lift*

For a required lift of 13.5N the wing should start the flight at configuration 1 or 2 for speed of 20m/s, morphing to configuration 2 at 25m/s, then morphing to configuration 5 at 35 m/s and finally to configuration 4 at 40m/s. At the end of the morphing process the drag reduction would be 26.3%, when the wing is at configuration 4 instead of configuration 2.

Note that on configurations 3 and 4, drag performance is not the one expected. When comparing the planform shapes of these configurations with configuration 5, their drag performance should be superior, since the areas are less or equal and the aspect ratio is higher than the ones of configuration 5. The reason why this is not so, is due to the increasing of wing's relative thickness when the chord is retracted, as well as the lower stretch level that the wing skin is submitted to in these configurations, that causes the skin to deform and alter the wing sections geometry more easily.

6- Synthesis

During the manufacturing process some conclusions were taken. Some components revealed to be non-functional. The spacing mechanism initially designed did not work. The reason for this was the tolerances involved; we found that the tolerances had to be very small. The connecting pins had to be tight enough for the space bars not to move freely, but at the same time the recess had to be enough to let the same bars move when needed. We had not enough precision to make this mechanism. As a result we replaced it for rubber bands connecting the ribs.

The rubber bands connecting the ribs were able to keep the same spacing between the ribs.

The leading and trailing edge blocks and beams initially thought to be in aluminium were made of acrylic. We made this change after the evaluation of the endurance of the aluminium. The whole structure initially was projected to be made of aluminium; however, having all components in the same material would cause fatigue. Another reason to change the material was the easiness to machine acrylic.

The wing's structure resulting was able to fulfil the requirements previously set.

Influence of stretch and stiffness of the wing's skin on the aerodynamics of the wing was studied. Increasing the wing's stretch helps approximate the wing to a rigid skin wing, therefore approximating the aerodynamics of the wing to what is usually seen in aerodynamics studies. The increase in skin stiffness helps to prevent the occurrence of skin instability at high speeds. However, higher skin's stiffness drives to a higher actuation force and higher loads upon the structure. As a result, the structure should be stronger, which increases the weight.

The results obtained on the wind tests of the morphing wing show that drag reductions up to 45% could be obtained with this wing, when we compare the take off wing with the high speed wing.

The results have showed that we were able to use a morphing mechanism to reduce drag, while maintaining the lift required. The reduction of drag is due to the reduction of wing area, since at higher speeds we can use smaller wings to produce the same lift.

Further work should be focus on improvement of the weakness revealed by our mechanism. A mechanism able to change actively the thickness and to make the airfoil thinner for higher speeds would be a very important development.